Effect of surface preparations on contact resistivity of TiW to highly doped n-InGaAs

Vibhor Jain[1], Ashish K. Baraskar[1], Mark A. Wistey[1,2], Uttam Singisetti[1], Zach Griffith[3], Evan Lobisser[1], Brian J. Thibeault[1], Arthur. C. Gossard[1,2], Mark. J. W. Rodwell[1]

[1]Electrical and Computer Engineering Department, University of California Santa Barbara, Santa Barbara, CA 93106-9560
[2]Materials Department, University of California Santa Barbara, Santa Barbara, CA 93106-5050
[3]Teledyne Scientific & Imaging, Thousand Oaks, CA 91360
Phone: (805) 893-8044, Email: vibhor@ece.ucsb.edu

Abstract

We report the effects of UV-ozone oxidation, oxide removal etch chemistry (dilute HCl or concentrated NH_4OH), semiconductor doping, and annealing on the contact resistivity (ρ_c) of $Ti_{0.1}W_{0.9}$ refractory alloy to n-type InGaAs. The semiconductor surface was oxidized through exposure to UV-ozone, then subsequently etched by either dilute HCl or concentrated NH_4OH before TiW contacts were deposited by blanket sputtering. InGaAs samples doped at 5×10^{19} cm^{-3}, treated with 10 minutes of UV-Ozone then one minute dilute HCl exhibited ρ_c of $(1.90 \pm 0.35) \times 10^{-8}$ Ω-cm^2. The contacts are thermally stable at least to 400 °C where after one minute anneal, ρ_c reduced to $(1.29 \pm 0.28) \times 10^{-8}$ Ω-cm^2. TiW contacts on samples having same active dopants, with no UV-ozone oxidation and only 10 seconds of concentrated NH_4OH etch exhibit ρ_c of $(2.49 \pm 0.40) \times 10^{-8}$ Ω-cm^2.

I. INTRODUCTION

High speed electronic devices require very low resistance metal semiconductor ohmic contacts which remain stable under high current bias and thermal stress as transistors are scaled towards THz bandwidths. Geometric scaling laws show that doubling transistor bandwidths requires a four-fold reduction in contact resistivity (ρ_c) (1-2). For simultaneous f_t and f_{max} of greater than 1-THz in InP HBTs, emitter and base contact resistivities less than 2×10^{-8} Ω-cm^2 are specified (3). InP FETs have similar requirements of low contact resistance for high speed operation (1).

Traditionally titanium (Ti) has been used to make low-resistance contacts to n-InGaAs. However, under thermal stress and cycling, Ti-based ohmic contacts deteriorate making Ti incompatible with high temperature processing and also raising concerns for high current density operations (4-5). Low resistance ohmic contacts to III-V semiconductors are attainable by alloying AuGe eutectic and semiconductor (6) but the semiconductor surfaces must be free of surface oxides and defects before metal deposition. Contact resistivity of 4.3×10^{-8} Ω-cm^2 has been reported on n-InGaAs by using an Ar^+ sputter clean of the surface prior to depositing Ti/Pt/Au contacts (7). Very low resistivity contacts exhibiting ρ_c of 0.5×10^{-8} Ω-cm^2 between Ti and n^+-InAs have been reported in (8) but the surface preparation procedures are not described. We previously reported that the n-InGaAs surfaces treated with UV-ozone plus concentrated NH_4OH could reduce contact resistivity without the use of Ti (5, 9). Follow up studies by secondary ion mass spectroscopy (SIMS) revealed that the reported samples contained a thin, unintentional layer of Ti (less than 1nm) at the metal (TiW)-semiconductor interface. In addition, InGaAs regrowth studies from our laboratory onto samples prepared using an NH_4OH rinse after UV-ozone treatment led to poor epitaxial regrowth, suggesting a substantial oxide layer was not removed. With this new data, we believe that Ti, rather than NH_4OH, is responsible for the low contact resistivity reported in (5).

Ex-situ contacts have been observed to be very sensitive to surface preparation techniques because the semiconductor surface rapidly becomes oxidized and/or contaminated in the time between surface preparation and metal deposition. In this paper we report a systematic study of how the resistivity of ex-situ refractory TiW contacts is affected by UV-ozone oxidation, oxide removal etch chemistry (dilute HCl or concentrated NH_4OH), n-type doping of semiconductor with Si and anneal temperature. Here, in the TiW metal contacts, thin interfacial metal layers are avoided in order to make the process more robust and reproducible. Additional studies were performed to ensure the absence of any unintentional interfacial metal layers for the results reported.

978-1-4244-3433-6/09/$25.00©2009 IEEE

II. FABRICATION

Structures shown in Fig. 1 were grown by solid source molecular beam epitaxy (MBE) on (100) semi-insulating InP substrates. The Si-doped InGaAs layer had an electron concentration varying from 5×10^{19} cm^{-3} to 5×10^{18} cm^{-3} for the wafers used as determined by Hall measurements. The samples were exposed to UV-ozone for varying times and then treated with either 60 seconds 1:10 HCl:H_2O and 60 seconds DI rinse (dilute HCl etch), or 10 seconds concentrated NH_4OH (14.8N) with no DI rinse (5). The samples were then immediately loaded for blanket Ar-sputtering deposition of TiW (90% W alloy). Blanket metal deposition avoids the lift-off step which exposes the semiconductor surface to photoresist. Photoresists tend to react with etchants used during surface preparation. Sometimes photoresist residue is also left after lithography which is removed by oxygen plasma that may cause damage to the semiconductor surface. Ti/Au/Ni (20/150/50 nm) was deposited by electron-beam evaporation and lifted off to define transmission line model (TLM) pads. With Ni as the etch mask, TiW was then etched in SF_6/Ar using inductively coupled plasma. Next, a wet etch was done to remove semiconductor down to semi-insulating InP and isolate the TLM patterns. A typical TLM pattern is shown in Fig 2. For annealing tests, samples were rapid thermal annealed for 60 seconds at 250-400 °C in N_2 environment.

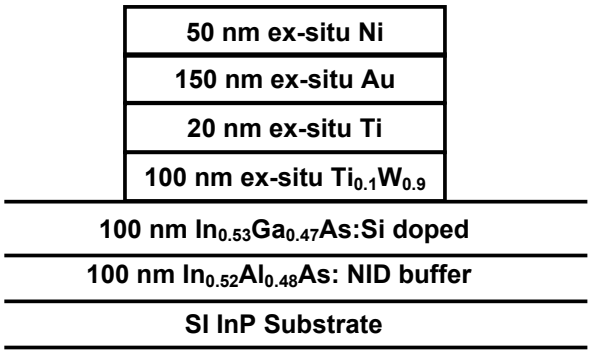

Fig 1: Cross-section schematic of the metal-semiconductor contact layer structure

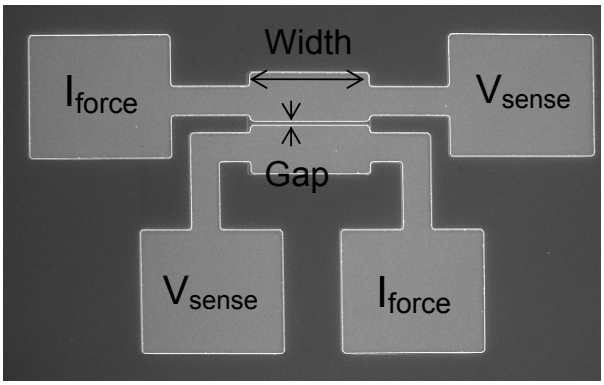

Fig 2: SEM image of the TLM pad with 600nm gap indicating the current source and voltage measurement pads

III. RESULTS AND ANALYSIS

Resistance was measured at room temperature on an Agilent 4155C semiconductor parameter analyzer using the four point probe technique to eliminate probe and interconnect parasitic resistances from the measurement. TLM pad spacing from 0.6-25 µm were verified using scanning electron microscopy (SEM). TLM contact pads are designed so that the resistance of the path common to current bias and voltage measurement is only measured. Thick metal pad (320 nm) on semiconductor reduces the effect of metal resistance on measurement. Interchanging the bottom pair of I_{force}-V_{sense} probes (Fig 2) caused less than 15% shift in measured contact resistivity. A plot of TLM resistance as a function of gap spacing for different surface treatments is shown in Fig 3. Sheet resistance and contact resistivity were calculated from the plot as mentioned in (10). Sheet resistance of the samples with NH_4OH and HCl treatment is different due to difference in carrier mobility data which resulted from different growth conditions (mobility ~ 870 $cm^2 V^{-1}s^{-1}$ for samples to be treated with dilute HCl and ~ 540 $cm^2 V^{-1}s^{-1}$ for those to be treated with concentrated NH_4OH). However, active dopant concentration is same for both the cases.

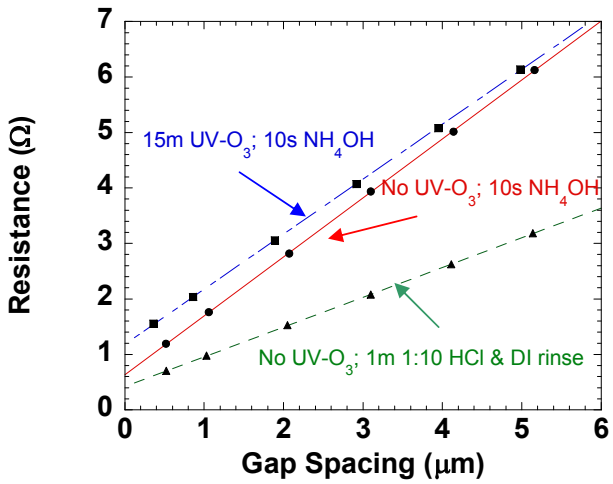

Fig 3: Measured resistance as a function of pad spacing for the contacts from 0.6µm to 6µm gap

A. UV-Ozone Oxidation and Etch Chemistry

The variation in contact resistivity with UV-ozone oxidation time for different etch chemistries is shown in Fig 4. Active dopant concentration for all these samples was kept same at 5

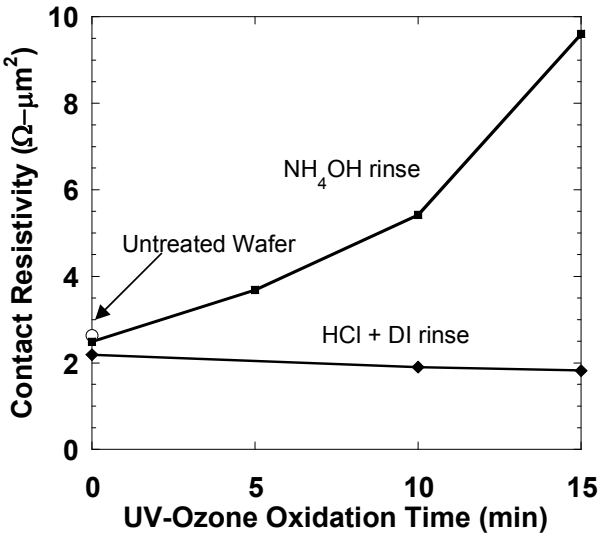

Fig 4: Contact resistivity variation with UV-ozone oxidation time for two different oxide-removal etch chemistries

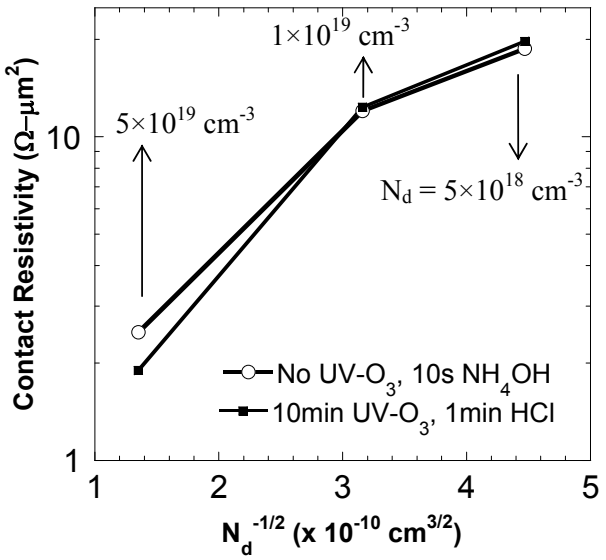

Fig 5: Contact resistivity (ρ_c) as a function of doping in the semiconductor for two different etch chemistries; ρ_c variation with N_d shows that dominant electron transport mechanism from metal to semiconductor is tunneling

$\times 10^{19}$ cm^{-3}. The contact resistivity for NH_4OH etched samples is observed to increase with oxidation time. It increases from $(2.49 \pm 0.40) \times 10^{-8}$ Ω-cm^2 with no oxidation to $(9.61 \pm 0.93) \times 10^{-8}$ Ω-cm^2 after 15 minutes of oxidation. XPS data also shows an increase in surface oxygen content from 26% to 41%. Therefore, NH_4OH etch is not sufficient to remove surface oxides formed during UV-ozone oxidation. Samples with an increased etch time and same oxidation time also exhibit similar contact resistivity. ρ_c of $(5.42 \pm 1.01) \times 10^{-8}$ Ω-cm^2 was measured for samples with 10 minutes UV-ozone and 10 seconds NH_4OH etch while 30 seconds long etch samples exhibited ρ_c of $(5.37 \pm 0.99) \times 10^{-8}$ Ω-cm^2. Therefore, even an extended concentrated NH_4OH etch is not effective in removing surface oxides in the case of long UV-Ozone oxidation (longer than 5 minutes based on the observed contact resistivities), causing an increase in the measured contact resistivity.

The contact resistivity for HCl samples was almost constant with oxidation time, indicating that the HCl etch removed oxides from the surface. This is also evident from XPS data where the surface oxygen content was found to be similar (~13-15%) for the same etch time but different oxidation times. Contact resistivity decreased slightly with increase in oxidation time, from $(2.19 \pm 0.38) \times 10^{-8}$ to $(1.82 \pm 0.34) \times 10^{-8}$ Ω-cm^2 (0 to 15 minute oxidation time). Although this slight decrease falls within the error margins, it could possibly be attributed to removal of hydrocarbon contamination by ozone followed by complete removal of the oxide by HCl. XPS analysis shows 7% reduction in surface carbon content after 15 minutes of UV-ozone.

The control sample, which had no surface treatment, showed a contact resistivity of $(2.63 \pm 0.43) \times 10^{-8}$ Ω-cm^2, comparable to samples with only NH_4OH or HCl etch rinse.

B. Doping

An increase in active dopants in the semiconductor results in a decrease in contact resistivity as shown in Fig 5. An order of magnitude decrease in doping from 5×10^{19} to 5×10^{18} cm^{-3} results in an increase in contact resistivity from $(1.90 \pm 0.35) \times 10^{-8}$ Ω-cm^2 to $(19.71 \pm 2.07) \times 10^{-8}$ Ω-cm^2 for 10 minute UV-Ozone, dilute HCl etch samples and from $(5.42 \pm 1.01) \times 10^{-8}$ Ω-cm^2 to $(18.70 \pm 2.00) \times 10^{-8}$ Ω-cm^2 for no UV-ozone & concentrated ammonia etch samples. This increase suggests that for the highest semiconductor doping concentrations the dominant electron transport mechanism from TiW into the semiconductor is tunneling (11). For higher electron concentration, a shallower depletion at the metal-semiconductor interface exists, thereby decreasing the tunneling resistance and consequently the contact resistivity. We have also observed that an increase in "inactive" dopants keeping the same carrier concentration also reduces contact resistivity (12).

C. Annealing

Contact resistivity as a function of annealing temperature has been plotted in Fig 6. It is observed that for both types of chemical etching, the contacts are stable even after anneal at 400 °C. After a one minute anneal at 400 °C, the contact resistivity for 10 minute UV-ozone, dilute HCl etch sample reduces from $(1.90 \pm 0.35) \times 10^{-8}$ Ω-cm^2 to $(1.29 \pm 0.28) \times 10^{-8}$ Ω-cm^2 and for 10 minute UV-ozone, concentrated ammonia etch from $(5.42 \pm 1.01) \times 10^{-8}$ Ω-cm^2 to $(2.89 \pm 0.71) \times 10^{-8}$ Ω-cm^2.

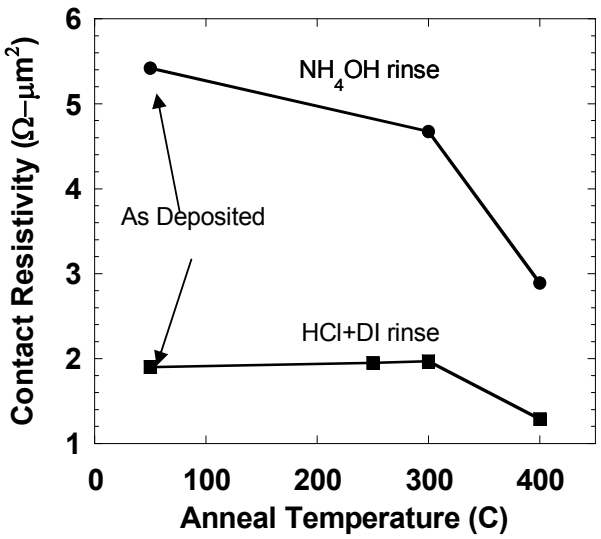

Fig 6: Variation in contact resistivity with annealing temperature for 1 minute anneal in N_2 environment

D. Error Analysis

Error analysis is done to estimate systematic error in the contact resistivity as mentioned in (13). For the error analysis, error in TLM gaps measured using SEM is taken as 20nm and in width as 0.2μm based on the resolution of the system. To estimate the random error in resistance measurements using the Agilent 4155C, repeated measurements (~100) on the same TLM pad were done at different current bias with varied probe placement location. This analysis estimates the error in resistance (dR) as 0.5mΩ. Assuming the worst case offsets in bias current and voltage (14), and including the random error calculated above, the value of dR is calculated to be less than 5mΩ. For a conservative estimate, dR is taken to be 50mΩ in the error analysis.

IV. CONCLUSION

In summary, we report low resistance, ex-situ, and refractory TiW metal contacts to n^+-InGaAs which are stable to at least 400 °C. For high electron concentration of 5×10^{19} cm^{-3} in n-InGaAs, 10 minutes of UV-ozone oxidation with one minute dilute HCl etch results in low contact resistivity of $(1.29 \pm 0.28) \times 10^{-8}$ Ω-cm^2 after one minute anneal at 400 °C. This resistivity is lower than the requisite value specified for greater than 1-THz f_{max} transistors and high current density operations. We observed that doping is the most important parameter that affects contact resistivity while different surface preparation techniques are of secondary influence. Dilute HCl etch is more effective in removing surface oxides compared to concentrated ammonia etch resulting in different contact resistivity variation trends with oxidation time for the two etchants. Thus, to obtain low contact resistivity, high doping in conjunction with an etch chemistry which fully removes surface oxides and annealing is required.

ACKNOWLEDGMENTS

This work was supported by the DARPA TFAST program N66001-02-C-8080. A portion of this work was done in the UCSB nanofabrication facility, part of the NSF funded NNIN network.

REFERENCES

(1) M.J.W. Rodwell, E. Lind, Z. Griffith, S.R. Bank, A.M. Cook, U. Singisetti, M. Wistey, G. Burek, A.C. Gossard; *IEEE 19th Int. Conf on Indium Phosphide & Related Materials, 2007.* pp.9-13, 14-18 May 2007

(2) M.J.W. Rodwell *et al.*; *IEEE Trans. on Electron Devices*, vol.48, no.11, pp.2606-2624, Nov 2001

(3) M.J.W. Rodwell *et al.; Compound Semiconductor Integrated Circuits Symp, 2008 CSICS '08*, pp.1-3, 12-15 Oct. 2008

(4) E.F. Chor, R.J. Malik, R.A. Hamm, R. Ryan; *Electron Device Letters, IEEE* , vol.17, no.2, pp.62-64, Feb 1996

(5) Adam M. Crook, Erik Lind, Zach Griffith, Mark J. W. Rodwell, Jeremy D. Zimmerman, Arthur C. Gossard, Seth R. Bank; *Appl. Phys. Lett.* 91, 192114, 2007

(6) N. Braslau; *J. of Vac. Sci. Technol,* 19(3), Sept/Oct 1981

(7) G. Stareev, H. Kunzel, G. Dortmann; *J of Appl. Phys*., vol. 74, no. 12, pp. 7344-7356, Dec 1993

(8) T. Nittono, H. Ito, O. Nakajima, T. Ishibashi; *Japanese J of Appl. Phys*., vol. 27, no. 9, pp. 1718-1722, Sept 1988

(9) U. Singisetti, A.M. Crook, E. Lind, J.D. Zimmerman, M.A. Wistey, A.C. Gossard, M.J.W. Rodwell; *Device Research Conf, 2007 65th Annual*, pp.149-150, 18-20 June 2007

(10) G.K. Reeves, H.B. Harrison; *IEEE Electron Devices Letters*, vol. EDL-3, no. 5, pp. 111-113, May 1982

(11) S.M. Sze, *Physics of Semiconductor Devices*, 2nd edition, pp 304-306

(12) Ashish K. Baraskar, M. Wistey, V. Jain, U. Singisetti, G. Burek, B.J. Thibeault, A.C. Gossard, M.J.W. Rodwell,; *36th Conf on the Phys and Chem of Surfaces and Interfaces, PCSI-36, Santa Barbara*, 11-15 Jan 2009

(13) H. Ueng, D.B. Janes, K.J Webb; *IEEE Trans on Electron Devices;* vol 48, no.4, pp. 758-766, Apr 2008

(14) Agilent 4155C Semiconductor Parameter Analyzer Data Sheet; http://cp.literature.agilent.com/litweb/pdf/5988-9238EN.pdf